Inorg. Chem. **2009**, *48*, 1148−1157

Synthesis, Structure, and Magnetism of Heterobimetallic Trinuclear Complexes {[L_2Co_2Ln][X]} [Ln = Eu, X = Cl; Ln = Tb, Dy, Ho, X = NO_3; LH_3 = (S)P[N(Me)N=CH−C_6H_3-2-OH-3-OMe]$_3$]: A 3d−4f Family of Single-Molecule Magnets

Vadapalli Chandrasekhar,*,† Balasubramanian Murugesa Pandian,† Jagadese J. Vittal,‡ and Rodolphe Clérac*,§,||

Department of Chemistry, Indian Institute of Technology—Kanpur, Kanpur-208016, India, Department of Chemistry, National University of Singapore, Singapore, CNRS, UPR 8641, Centre de Recherche Paul Pascal (CRPP), Equipe "Matériaux Moléculaires Magnétiques", 115 avenue du Dr. Albert Schweitzer, Pessac, F-33600, France, and Université de Bordeaux, UPR 8641, Pessac, F-33600, France

Received October 7, 2008

Sequential reaction of LH_3 (LH_3 = (S)P[N(Me)N=CH−C_6H_3-*2*-OH-*3*-OMe]$_3$) with $Co(OAc)_2 \cdot 4H_2O$ followed by reaction with lanthanide salts afforded trinuclear heterobimetalllic compounds {[L_2Co_2Ln][X]} [Ln = Eu (**1**), X = Cl; Ln = Tb (**2**), Dy (**3**), Ho (**4**), X = NO_3] in excellent yields. These compounds retain their integrity in solution as determined by electrospray ionization mass spectrometry studies. The molecular structures of **1**−**4** were confirmed by a single-crystal X-ray structural study and reveal that these are isostructural. In all of the compounds, the three metal ions are arranged in a perfectly linear manner and are held together by two trianionic ligands, L^{3-}. The two terminal Co^{II} ions contain a facial coordination environment (3N, 3O) comprising three imino nitrogen atoms and three phenolate oxygen atoms. The coordination geometry about the cobalt atom is severely distorted. An all-oxygen coordination environment (12O) is present around the central lanthanide ion, which is present in a distorted icosahedral geometry. The coordination sphere around the lanthanide ion is achieved by utilizing three phenolate oxygen atoms and three methoxy oxygen atoms of each ligand. In all of these trinuclear complexes (**1**−**4**), the Co−Ln distances are around 3.3 Å, while the Co−Co distances range from 6.54 to 6.60 Å. The screw-type coordination mode imposed by the ligand induces chirality in the molecular structure, although all of the complexes crystallize as racemates. Magnetic properties of **1**−**4** have been studied in detail using dc and ac susceptibility measurements. Dynamic measurements reveal that **2**−**4** display a single-molecule magnet behavior, while the Co_2Eu (**1**) analogue does not show any out-of-phase ac susceptibility.

Introduction

In recent years, coordination chemists have reported a considerable amount of work in the area of single-molecule magnets (SMMs).[1−5] At low temperatures, these molecular magnets exhibit slow relaxation of their magnetization induced by a combined effect of their uniaxial anisotropy and high-spin ground state (S_T). These two characteristics

* To whom correspondence should be addressed. Fax: (+91)-512-2597436 (V.C.), (+33) 5 56 84 56 00 (R.C.). E-mail: vc@iitk.ac.in (V.C.), clerac@crpp-bordeaux.cnrs.fr (R.C.).
† Indian Institute of Technology—Kanpur.
‡ National University of Singapore.
§ CRPP.
|| Université de Bordeaux.

(1) (a) Galloway, K. W.; Whyte, A. M.; Wernsdorfer, W.; Sanchez-Benitez, J.; Kamenev, K. V.; Parkin, A.; Peacock, R. D.; Murrie, M. *Inorg. Chem.* **2008**, *47*, 7438–7442. (b) Yoshihara, D.; Karasawa, S.; Koga, N. *J. Am. Chem. Soc.* **2008**, *130*, 10460–10461. (c) Zaleski, C. M.; Weng, T.-C.; Dendrinou-Samara, C.; Alexiou, M.; Kanakaraki, P.; Hsieh, W.-Y.; Kampf, J.; Penner-Hahn, J. E.; Pecoraro, V. L.; Kessissoglou, D. P. *Inorg. Chem.* **2008**, *47*, 6127–6136. (d) Stamatatos, T. C.; Poole, K. M.; Abboud, A. K.; Wernsdorfer, W.; O'Brien, T. A.; Christou, G. *Inorg. Chem.* **2008**, *47*, 5006–5021. (e) Ma, Y.-S.; Li, Y.-Z.; Song, Y.; Zheng, L.-M. *Inorg. Chem.* **2008**, *47*, 4536–4544. (f) Okazawa, A.; Nogami, T.; Nojiri, H.; Ishida, T. *Chem. Mater.* **2008**, *20*, 3110–3119. (h) Mishra, A.; Pushkar, Y.; Yano, J.; Yachandra, V. K.; Wernsdorfer, W.; Abboud, K. A.; Christou, G. *Inorg. Chem.* **2008**, *47*, 1940–1948.

10.1021/ic801905p CCC: $40.75
Published on Web 01/07/2009

create an energy barrier (Δ) between the two thermodynamically equivalent spin configurations, $m_S = \pm S_T$. Hence, below the so-called blocking temperature (T_B), the thermal energy is no longer able to overcome the barrier Δ, and the spin is trapped in one of the two equivalent configurations. This molecular property can be detected at the bulk level when a magnetic field is applied, saturating the magnetization below T_B. When this field is switched off, the magnetization slowly relaxes with a characteristic relaxation time (τ) that can be measured as a function of the temperature using the time dependence of the magnetization or the frequency dependence of the ac susceptibility. This slow relaxation of the magnetization leads at a low enough temperature to hysteresis effects with an applied field, which is the signature of magnetlike behavior.[6] The potential applications of SMMs are vast. These include information processing, data storage, quantum computing, spintronics, biomedical applications (like MRI contrast agents), or magnetic refrigeration.[7] In general, SMMs can be obtained by assembling polynuclear metal complexes containing high-spin metal ions and those that possess magnetic anisotropy. A classic example which combines the two features discussed above is the dodecanuclear manganese complex $[Mn_{12}O_{12}(CH_3COO)_{16}(H_2O)_4]$.[8]

Alternative synthetic strategies for preparation of SMMs include metal complexes containing 3d and 4f metal ions. In particular, Dy^{III} and Tb^{III} lanthanide ions with large spin and high spin−orbit coupling have been used in combination with some transition metal ions [Cu_2Tb_2, Dy_6Mn_6, Dy_4Mn_{11}, Dy_2Cu, Dy_3Cu_3, Dy_2Mn_2, FeDy, etc.] to afford SMMs.[9,10] Even some homometallic complexes containing these lanthanide ions have been shown to exhibit slow relaxation of the magnetization related to single-molecule magnet behavior.[11] Recently, in a radically different approach, we exploited the combination of the magnetic anisotropy of Co^{II} and the high-spin of Gd^{III} to report the first Co/Ln SMM {[L_2Co_2Gd][NO_3]}.[12] This result spurred us to explore the

(2) (a) Hiraga, H.; Miyasaka, H.; Nakata, K.; Kajiwara, T.; Takaishi, S.; Oshima, Y.; Nojiri, H.; Yamashita, M. *Inorg. Chem.* **2007**, *46*, 9661–9671. (b) Bagai, R.; Wernsdorfer, W.; Abboud, K. A.; Christou, G. *J. Am. Chem. Soc.* **2007**, *129*, 12918–12919. (c) Brockman, J. T.; Stamatatos, T. C.; Wernsdorfer, W.; Abboud, K. A.; Christou, G. *Inorg. Chem.* **2007**, *46*, 9160–9171. (d) Lecren, L.; Wernsdorfer, W.; Li, Y.-G.; Vindigni, A.; Miyasaka, H.; Clérac, R. *J. Am. Chem. Soc.* **2007**, *129*, 5045–5051. (e) Mishra, A.; Tasiopoulos, A. J.; Wernsdorfer, W.; Abboud, K. A.; Christou, G. *Inorg. Chem.* **2007**, *46*, 3105–3115. (f) Jiang, L.; Choi, H. J.; Feng, X.-L.; Lu, T.-B.; Long, J. R. *Inorg. Chem.* **2007**, *46*, 2181–2186. (g) Milios, C. J.; Vinslava, A.; Wernsdorfer, W.; Moggach, S.; Parsons, S.; Perlepes, S. P.; Christou, G.; Brechin, E. K. *J. Am. Chem. Soc.* **2007**, *129*, 2754–2755. (h) Freedman, D. E.; Jenkins, D. M.; Iavarone, A. T.; Long, J. R. *J. Am. Chem. Soc.* **2008**, *130*, 2884–2885.

(3) (a) Brechin, E. K.; Boskovic, C.; Wernsdorfer, W.; Yoo, J.; Yamaguchi, A.; Sanudo, E. C.; Concolino, T. R.; Rheingold, A. L.; Ishimoto, H.; Hendrickson, D. N.; Christou, G. *J. Am. Chem. Soc.* **2002**, *124*, 9710–9711. (b) Tassiopoulos, A. J.; Vinslave, A.; Wernsdorfer, W.; Abboud, K. A.; Christou, G. *Angew. Chem., Int. Ed.* **2004**, *43*, 2117–2121. (c) Schelter, E. J.; Prosvirin, A. V.; Dunbar, K. R. *J. Am. Chem. Soc.* **2004**, *126*, 15004–15005. (d) Beltran, L. M. C.; Long, J. R. *Acc. Chem. Res.* **2005**, *38*, 325–334. (e) Schelter, E. J.; Karadas, F.; Avendano, C.; Prosvirin, A. V.; Wernsdorfer, W.; Dunbar, K. R. *J. Am. Chem. Soc.* **2007**, *129*, 8139–8149. (f) Milios, C. J.; Inglis, R.; Vinslava, A.; Bagai, R.; Wernsdorfer, W.; Parsons, S.; Perlepes, S. P.; Christou, G.; Brechin, E. K. *J. Am. Chem. Soc.* **2007**, *129*, 12505–12511.

(4) (a) Sun, Z.; Grant, C. M.; Castro, S. L.; Hendrickson, D. N.; Christou, G. *Chem. Commun.* **1998**, 721–722. (b) Oshio, H.; Hoshino, N.; Ito, T. *J. Am. Chem. Soc.* **2000**, *122*, 12602–12603. (c) Murrie, M.; Stöeckli-Evans, H.; Güdel, H. U. *Angew. Chem., Int. Ed.* **2001**, *40*, 1957–1960. (d) Andres, H.; Basler, R.; Blake, A. J.; Cadiou, C.; Chaboussant, G.; Grant, C. M.; Güdel, H.-U.; Murrie, M.; Parsons, S.; Paulsen, C.; Semadini, F.; Villar, V.; Wernsdorfer, W.; Winpenny, R. E. P. *Chem.—Eur. J.* **2002**, *8*, 4867–4876. (e) Dendrinou-Samara, C.; Alexiou, M.; Zaleski, C. M.; Kampf, J. W.; Kirk, M. L.; Kessissoglou, D. P.; Pecoraro, V. L. *Angew. Chem., Int. Ed.* **2003**, *42*, 3763–3766. (f) Langley, S. J.; Helliwell, M.; Sessoli, R.; Rosa, P.; Wernsdorfer, W.; Winpenny, R. E. P. *Chem. Commun.* **2005**, 5029–5031. (g) Ishikawa, N.; Otsuka, S.; Kaizu, Y. *Angew. Chem., Int. Ed.* **2005**, *44*, 731.

(5) (a) Oshio, H.; Nihei, M.; Koizumi, S.; Shiga, T.; Nojiri, H.; Nakano, M.; Shirakawa, N.; Akatsu, M. *J. Am. Chem. Soc.* **2005**, *127*, 4568–4569. (b) Li, D.; Parkin, S.; Wang, G.; Yee, G. T.; Clérac, R.; Wernsdorfer, W.; Holmes, S. M. *J. Am. Chem. Soc.* **2006**, *128*, 4214–4215. (c) Kachi-Terajima, C.; Miyasaka, H.; Sugiura, K.-i.; Clérac, R.; Nojiri, H. *Inorg. Chem.* **2006**, *45*, 4381–4390.

(6) (a) Christou, G.; Gatteschi, D.; Hendrickson, D. N.; Sessoli, R. *MRS Bull.* **2000**, *25*, 66–71. (b) Gatteschi, D.; Sessoli, R. *Angew. Chem., Int. Ed.* **2003**, *42*, 268–297.

(7) (a) Wernsdorfer, W.; Sessoli, R. *Science* **1999**, *284*, 133–135. (b) Leuenberger, M. N.; Loss, D. *Nature* **2001**, *410*, 789–793. (c) Bogani, L.; Wernsdorfer, W. *Nat. Mater.* **2008**, *7*, 179–186. (d) Coronado, E.; Gatteschi, D. *J. Mater. Chem.* **2006**, *16*, 2513–2515. (e) Tejada, J.; Chudnovsky, E. M.; del Barco, E.; Hernandez, J. M.; Spiller, T. P. *Nanotechnology* **2001**, *12*, 181–186. (f) Cornia, A.; Constantino, A. F.; Zobbi, L.; Caneschi, A.; Gatteschi, D.; Mannini, M.; Sessoli, R. *Struct. Bonding (Berlin)* **2006**, *122*, 133–161, and references therein. (g) Gomez-Segura, J.; Veciana, J.; Ruiz-Molina, D. *Chem. Commun.* **2007**, 3699–3707. (h) Cage, B.; Russek, S. R.; Shoemaker, R.; Barker, A. J.; Stoldt, C.; Ramachandran, V.; Dalal, N. S. *Polyhedron* **2007**, *26*, 2413–2419. (i) Manoli, M.; Collins, A.; Parsons, S.; Candini, A.; Evangelisti, M.; Brechin, E. K. *J. Am. Chem. Soc.* **2008**, *130*, 11129–11139.

(8) (a) Boyd, P. D. W.; Li, Q.; Vincent, J. B.; Folting, K.; Chang, H.-R.; Streib, W. E.; Huffman, J. C.; Christou, G.; Hendrickson, D. N. *J. Am. Chem. Soc.* **1988**, *110*, 8537–8539. (b) Caneschi, A.; Gatteschi, D.; Sessoli, R.; Barra, A. L.; Brunel, L. C.; Guillot, M. *J. Am. Chem. Soc.* **1991**, *113*, 5873–5874. (c) Sessoli, R.; Tsai, H.-L.; Schake, A. R.; Wang, S.; Vincent, J. B.; Folting, K.; Gatteschi, D.; Christou, G.; Hendrickson, D. N. *J. Am. Chem. Soc.* **1993**, *115*, 1804–1816.

(9) (a) Zaleski, C. M.; Depperman, E. C.; Kampf, J. W.; Kirk, M. L.; Pecoraro, V. L. *Angew. Chem., Int. Ed.* **2004**, *43*, 3912–3914. (b) Osa, S.; Kido, T.; Matsumoto, N.; Re, N.; Pochaba, A.; Mrozinski, J. *J. Am. Chem. Soc.* **2004**, *126*, 420–421. (c) Mishra, A.; Wernsdorfer, W.; Abboud, K. A.; Christou, G. *J. Am. Chem. Soc.* **2004**, *126*, 15648–15649. (d) He, F.; Tong, M.-L.; Chen, X.-M. *Inorg. Chem.* **2005**, *44*, 8285–8292. (e) Mishra, A.; Wernsdorfer, W.; Parsons, S.; Christou, G.; Brechin, E. K. *Chem. Commun.* **2005**, 2086–2088. (f) Costes, J.-P.; Dahan, F.; Wernsdorfer, W. *Inorg. Chem.* **2006**, *45*, 5–7. (g) Costes, J.-P.; Auchel, M.; Dahan, F.; Peyrou, V.; Shova, M.; Wernsdorfer, W. *Inorg. Chem.* **2006**, *45*, 1924–1934. (h) Mori, F.; Nyui, T.; Ishida, T.; Nogami, T.; Choi, K.-Y.; Nojiri, H. *J. Am. Chem. Soc.* **2006**, *128*, 1440–1441. (i) Aronica, C.; Pilet, G.; Chastanet, G.; Wernsdorfer, W.; Jacquot, J.-F.; Luneau, D. *Angew. Chem., Int. Ed.* **2006**, *45*, 4659–4662. (j) Ferbinteanu, M.; Kajiwara, T.; Choi, K.-Y.; Nojiri, H.; Nakamoto, A.; Kojima, N.; Cimpoesu, F.; Fujimura, Y.; Takaishi, S.; Yamashita, M. *J. Am. Chem. Soc.* **2006**, *128*, 9008–9009. (k) Murugesu, M.; Mishra, A.; Wernsdorfer, W.; Abboud, K. A.; Christou, G. *Polyhedron* **2006**, *25*, 613–625.

(10) (a) Pointillart, F.; Bernot, K.; Sessoli, R.; Gatteschi, D. *Chem.—Eur. J.* **2007**, *13*, 1602–1609. (b) Mereacre, V. M.; Ako, A. M.; Clérac, R.; Wernsdorfer, W.; Filoti, G.; Bartolome, J.; Anson, C. E.; Powell, A. K. *J. Am. Chem. Soc.* **2007**, *129*, 9248–9249. (c) Zaleski, C. M.; Kampf, J. W.; Mallah, T.; Kirk, M. L.; Pecoraro, V. L. *Inorg. Chem.* **2007**, *46*, 1954–1956. (d) Hamamatsu, T.; Yabe, K.; Towatari, M.; Osa, S.; Matsumoto, N.; Re, N.; Pochaba, A.; Mrozinski, J.; Gallani, J.-L.; Barla, A.; Imperia, P.; Paulsen, C.; Kappler, J.-P. *Inorg. Chem.* **2007**, *46*, 4458–4468. (e) Mereacre, V.; Ako, A. M.; Clérac, R.; Wernsdorfer, W.; Hewitt, E. J.; Anson, C. E.; Powell, A. K. *Chem.—Eur. J.* **2008**, *14*, 3577–3584.

(11) (a) Ishikawa, N.; Sugita, M.; Ishikawa, T.; Koshihara, S.; Kaizu, Y. *J. Am. Chem. Soc.* **2003**, *125*, 8694–8695. (b) Ishikawa, N.; Sugita, M.; Ishikawa, T.; Koshihara, S.; Kaizu, Y. *J. Phys. Chem. B* **2004**, *108*, 11265–11271. (c) Sugita, M.; Ishikawa, N.; Ishikawa, T.; Koshihara, S.; Kaizu, Y. *Inorg. Chem.* **2006**, *45*, 1299–1304. (d) Tang, J.; Hewitt, I.; Madhu, N. T.; Chastanet, G.; Wernsdorfer, W.; Anson, C. E.; Benelli, C.; Sessoli, R.; Powell, A. K. *Angew. Chem., Int. Ed.* **2006**, *45*, 1729–1733. (e) Gamer, M. T.; Lan, Y.; Roesky, P. W.; Powell, A. K.; Clérac, R. *Inorg. Chem.* **2008**, *47*, 6581–6583.

Table 1. Crystal and Refinement Data for **1**−**4**

	1	2	3	4
empirical formula	$C_{57}H_{66}Cl_7Co_2EuN_{12}O_{13}P_2S_2$	$C_{56}H_{66}Cl_6Co_2TbN_{13}O_{17}P_2S_2$	$C_{56}H_{66}Cl_6Co_2DyN_{13}O_{17}P_2S_2$	$C_{56}H_{62}Cl_6Co_2HoN_{13}O_{15}P_2S_2$
fw	1771.25	1808.76	1812.34	1778.74
temperature (K)	100(2)	100(2)	100(2)	223(2)
wavelength (Å)	0.71073	0.71073	0.71073	0.71073
cryst syst	triclinic	triclinic	triclinic	triclinic
space group	$P\bar{1}$	$P\bar{1}$	$P\bar{1}$	$P\bar{1}$
unit cell dimensions (Å, deg)	a = 11.9098(10)	a = 11.5880(19)	a = 11.4217(18)	a = 11.4991(14)
	b = 16.3470(13)	b = 11.7744(19)	b = 12.1315(19)	b = 12.230(2)
	c = 19.0057(15)	c = 15.855(3)	c = 15.649(2)	c = 15.7517(19)
	α = 69.8330(10)	α = 71.553(3)	α = 84.513(3)	α = 84.047(3)
	β = 88.4610(10)	β = 86.256(3)	β = 72.507(3)	β = 72.1297(2)
	γ = 89.6400(10)	γ = 61.042(2)	γ = 62.187(3)	γ = 61.980(2)
volume (Å^3)	3475.0(5)	1785.5(5)	1826.5(5)	1859.1(4)
Z	2	1	1	1
density, calcd (g cm^{-3})	1.693	1.682	1.648	1.589
abs coeff (mm^{-1})	1.807	1.841	1.854	1.877
F(000)	1788	912	913	894
cryst size (mm^3)	0.10 × 0.08 × 0.06	0.25 × 0.16 × 0.14	0.10 × 0.09 × 0.08	0.35 × 0.30 × 0.18
θ range (deg)	2.03 to 25.00	2.02 to 25.99	2.09 to 26.00	2.07 to 25.00
limiting indices	$-14 \le h \le 14$	$-14 \le h \le 14$	$-14 \le h \le 12$	$-13 \le h \le 13$
	$-16 \le k \le 19$	$-13 \le k \le 14$	$-14 \le k \le 14$	$-14 \le k \le 14$
	$-22 \le l \le 21$	$-10 \le l \le 19$	$-19 \le l \le 19$	$-10 \le l \le 18$
reflns collected	17917	10054	10349	10710
ind reflns	12012 [R(int) = 0.0271]	6870 [R(int) = 0.0266]	7005 [R(int) = 0.0375]	6515 [R(int) = 0.0250]
completeness to θ (%)	98.1	97.8	97.8	99.1
refinement method	full-matrix least-squares on F^2	full-matrix least-squares on F^2	full-matrix least-squares on F^2	full-matrix least-squares on F^2
data/restraints/params	12012/0/871	6870/456/493	7005/470/488	6515/32/450
goodness-of-fit on F^2	1.059	1.022	1.063	1.075
Final R indices [$I > 2\theta(I)$]	R1 = 0.0512, wR2 = 0.1338	R1 = 0.0483, wR2 = 0.1256	R1 = 0.0598, wR2 = 0.1511	R1 = 0.0567, wR2 = 0.1655
R indices (all data)	R1 = 0.0621, wR2 = 0.1466	R1 = 0.0571, wR2 = 0.1322	R1 = 0.0749, wR2 = 0.1600	R1 = 0.0679, wR2 = 0.1740
largest diff. peak and hole (e•Å^{-3})	3.186 and −1.494	1.979 and −0.815	1.865 and −0.707	1.753 and −1.647

Scheme 1

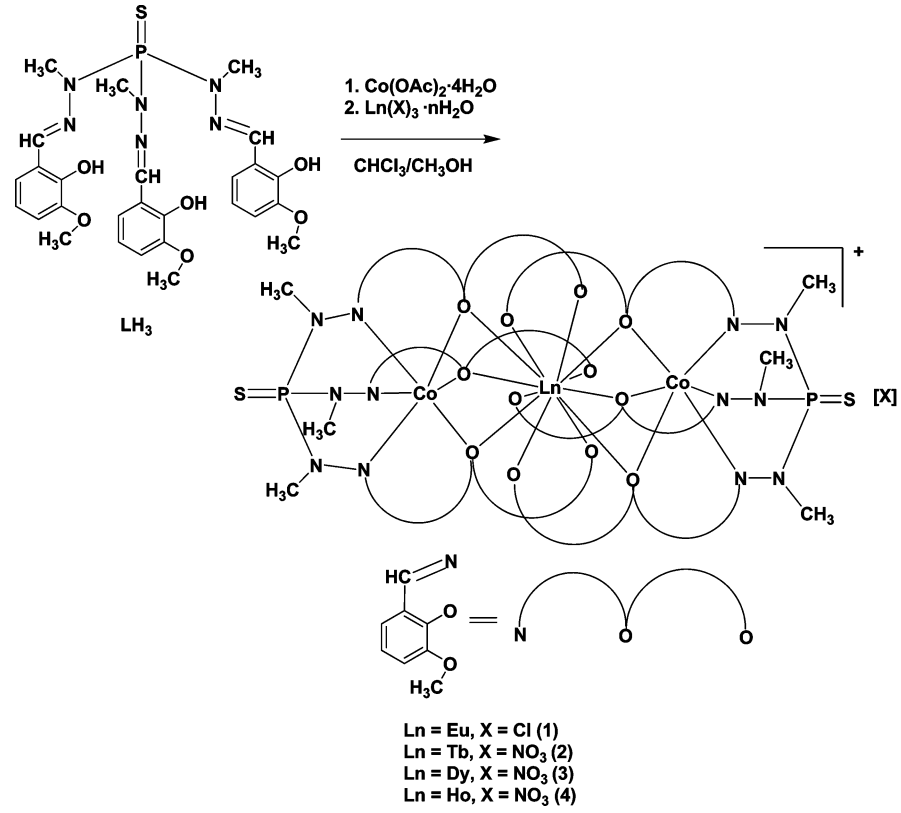

combination of Co^{II} with other lanthanide ions and especially those that possess magnetic anisotropy such as Dy^{III}, Ho^{III}, and Tb^{III} ions. For comparison, we also examined the incorporation of Eu^{III}. Accordingly, we report in this paper

the synthesis, structural characterization studies, and detailed magnetic properties of a new family of complexes: {[L_2Co_2Ln][X]} [LH_3 = (S)P[N(Me)N=CH−C_6H_3-2-OH-3-OMe]$_3$; Ln = Eu, X = Cl (**1**); Ln = Tb, X = NO_3 (**2**); Ln = Dy, X = NO_3 (**3**); Ln = Ho, X = NO_3 (**4**)], and the discovery of the SMM behavior of **2**, **3**, and **4**.

Experimental Section

Reagents and General Procedures. Solvents and other general reagents used in this work were purified according to standard procedures.[13] $P(S)Cl_3$ and 3-methoxy salicylaldehyde (Fluka, Switzerland) were used as purchased. N-Methylhydrazine was obtained as a gift from Vikram Sarabhai Space Research Centre, Thiruvananthapuram, India, and used as such. LH_3 was synthesized by a literature procedure.[12] $Co(OAc)_2 \cdot 4H_2O$ was obtained from S.D. Fine Chemicals, Mumbai, India. $EuCl_3 \cdot 6H_2O$, $Dy(NO_3)_3 \cdot 5H_2O$, $Ho(NO_3)_3 \cdot 5H_2O$, and $Tb(NO_3)_3 \cdot 5H_2O$ were obtained from Sigma Aldrich Chemical Co. and used as received.

Instrumentation. Melting points were measured using a JSGW melting point apparatus and are uncorrected. IR spectra were recorded as KBr pellets on a Bruker Vector 22 FT IR spectrophotometer operating at 400−4000 cm^{-1}. Elemental analyses of the compounds were obtained from Thermoquest CE instruments CHNS-O, EA/110 model. Electrospray ionization mass spectrometry (ESI-MS) spectra were recorded on a Micromass Quattro II triple quadrupole mass spectrometer.

Magnetic Measurements. Magnetic susceptibility measurements were obtained with the use of a Quantum Design SQUID magnetometer MPMS-XL. This magnetometer works between 1.8 and 400 K for dc applied fields ranging from −7 to +7 T. Measurements were performed on finely ground crystalline samples. *M* versus *H* measurements were performed at 100 K to check for the presence of ferromagnetic impurities which were found to be absent. ac susceptibility measurements were measured using an oscillating ac field of 3 Oe with ac frequencies ranging from 1 to 1500 Hz. Magnetic data were corrected for the sample holder and the diamagnetic contribution.

X-Ray Crystallography. Crystal data and cell parameters for compounds **1**−**4** are given in Table 1. Single crystals suitable for X-ray crystallographic analyses were obtained by a slow diffusion of *n*-hexane into a solution of **1**−**4** in a chloroform/methanol mixture. Crystal data for compounds **1**−**4** were collected on a Bruker SMART CCD diffractometer using a Mo Kα sealed tube. The program SMART[14a] was used for collecting frames of data, indexing reflections, and determining lattice parameters; SAINT[14a] for integration of the intensity of reflections and scaling; SADABS[14b] for absorption correction; and SHELXTL[14c,d] for space group and structure determination and least-squares refinements on F^2. All structures were solved by direct methods using the program SHELXS-97[14e] and refined by full-matrix least-squares methods against F^2 with SHELXL-97.[14e] Hydrogen atoms were fixed at calculated positions, and their positions were refined by a riding model. All non-hydrogen atoms were refined with anisotropic displacement parameters. In compound **1**, methanol was refined isotropically. In compound **2**, the hydrazone nitrogen, imino, and N-methyl carbon atom were found to be disordered. These atoms (50/50) were refined isotropically, and the disordered chloroform solvent and nitrate anion also were refined isotropically. In **3**, disordered water was refined isotropically. In **4**, one half of a nitrate ion in the asymmetric unit was found to be disordered. Two disordered nitrate ions (50/50) were resolved isotropically.

Synthesis

Preparation of the Trinuclear Metal Complexes 1−4. The general procedure for the preparation of the metal complexes is as follows. LH_3 (0.20 g, 0.333 mmol) was taken in a mixture of chloroform (30 mL) and methanol (30 mL). $Co(OAc)_2 \cdot 4H_2O$ (0.08 g, 0.321 mmol) was added to this solution. The reaction mixture was stirred for about 5 min. At this stage, $LnX_3 \cdot nH_2O$ (0.167 mmol) [X = Cl for **1** and NO_3 for **2**−**4**] was added, and the reaction mixture was stirred for a further period of 12 h to afford a clear solution. This was filtered and the filtrate evaporated to dryness. The residue obtained was washed with *n*-hexane and dried and was identified as the trinuclear complex. All of the complexes, thus obtained, were purified by crystallization using conditions as described in the section on X-ray crystallography. The characterization data for these complexes are given below.

[{(S)P[N(Me)N=CH−C_6H_3-2-O-3-OMe]$_3$}$_2$$Co_2$Eu]Cl·2$CHCl_3$·$CH_3OH$ (1). Yield: 0.220 g, 73.4%. Mp: >280 °C. FT-IR ν/cm^{-1}: 1601 (C=N). ESI-MS: 1465.12 $(M)^+$. Anal. calcd for $C_{57}H_{66}Cl_7Co_2EuN_{12}O_{13}P_2S_2$: C, 38.65; H, 3.76; N, 9.49; S, 3.62. Found: C, 38.02; H, 3.69; N, 9.32; S, 3.50.

[{(S)P[N(Me)N=CH−C_6H_3-2-O-3-OMe]$_3$}$_2$$Co_2$Tb]$NO_3$·2$CHCl_3$·2$H_2O$ (2). Yield: 0.218 g, 72.2%. Mp: >280 °C. FT-IR ν/cm^{-1}: 1597 (C=N), 1384 (NO_3). ESI-MS: 1471.13$(M)^+$. Anal. calcd for $C_{56}H_{66}Cl_6Co_2TbN_{13}O_{17}P_2S_2$: C, 37.18; H, 3.68; N, 10.07; S, 3.55. Found: C, 36.88; H, 3.60; N,10.29; S, 3.40.

[{(S)P[N(Me)N=CH−C_6H_3-2-O-3-OMe]$_3$}$_2$$Co_2$Dy]$NO_3$·2$CHCl_3$·2$H_2O$ (3). Yield: 0.225 g, 74.6%. Mp: >280 °C. FT-IR ν/cm^{-1}: 1599 (C=N), 1384 (NO_3). ESI-MS: 1476.14 $(M)^+$. Anal. calcd for $C_{56}H_{66}Cl_6Co_2DyN_{13}O_{17}P_2S_2$: C, 37.11; H, 3.67; N, 10.05; S, 3.54. Found: C, 36.92; H, 3.49; N, 9.82; S, 3.44.

[{(S)P[N(Me)N=CH−C_6H_3−2-O-3-OMe]$_3$}$_2$$Co_2$Ho]$NO_3$·2$CHCl_3$ (4). Yield: 0.210 g, 71.65%. Mp: >280 °C. FT-IR ν/cm^{-1}: 1599 (C=N), 1385 (NO_3). ESI-MS: 1477.14 $(M)^+$. Anal. calcd for $C_{56}H_{62}Cl_6Co_2HoN_{13}O_{15}P_2S_2$: C, 37.81; H, 3.51; N, 10.24; S, 3.60. Found: C, 36.92; H, 3.39; N, 9.92; S, 3.50.

Results and Discussion

In a preliminary communication,[12] we have reported the utilization of the phosphorus-supported ligand LH_3 for the preparation of heterobimetallic compounds. The interesting aspect of LH_3 is that it possesses nine coordination sites. Six of those sites, three imino nitrogen atoms and three phenolate oxygen atoms, are strongly coordinating, while three others, namely, the oxygen atoms of the −OMe group, are weakly coordinating. However, the latter have sufficient binding capacity toward lanthanide metal ions. Sequential reaction of LH_3 with $Co(OAc)_2 \cdot 4H_2O$ followed by reaction with the appropriate lanthanide salt afforded trinuclear heterobimetallic compounds **1**−**4** in about 70% yield (Scheme 1). All of these complexes showed a molecular ion peak in their ESI-MS spectrum (see Experimental Section), in agreement with the expected structure already observed in {[L_2Co_2Gd][NO_3]}.[12] The molecular structures of **1**−**4** were confirmed by their single-crystal X-ray structural study, as described below.

(12) Chandrasekhar, V.; Pandian, B. M.; Azhakar, R.; Vittal, J. J.; Clérac, R. *Inorg. Chem.* **2007**, *46*, 5140–5142.
(13) Furniss, B. S.; Hannaford, A. J.; Smith, P. W. G.; Tatchell, A. R. *Vogel's Textbook of Practical Organic Chemistry*, 5th ed.; ELBS, Longman: London, 1989.

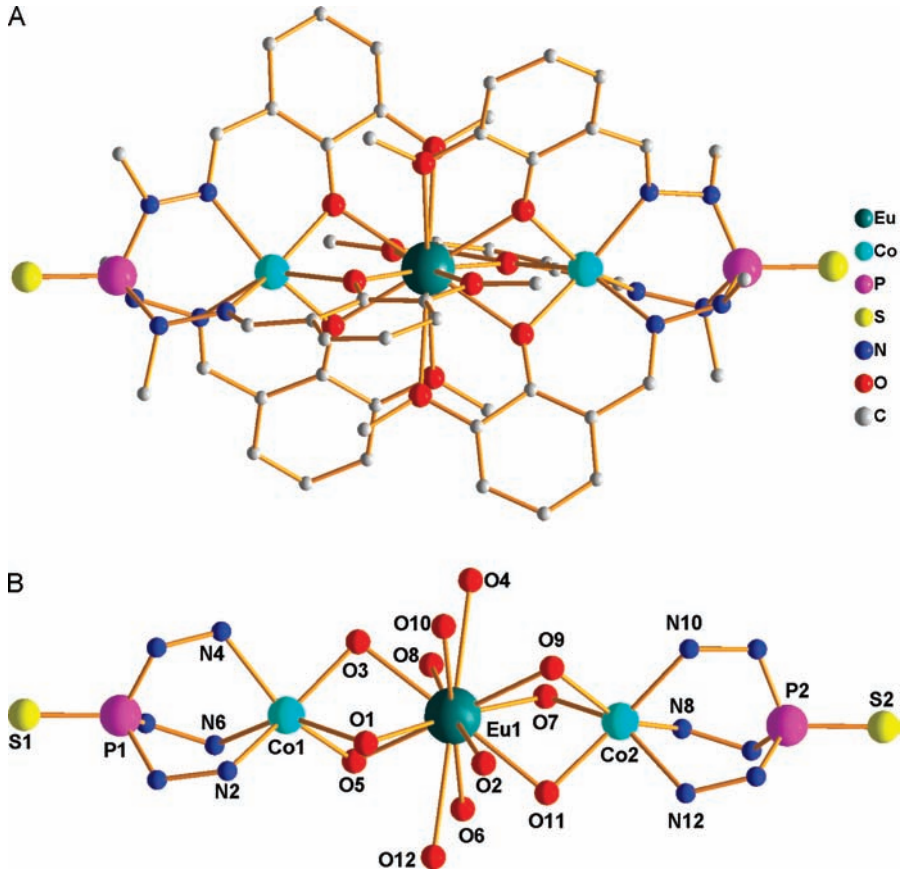

Figure 1. (A) Cationic portion of **1**. All hydrogen atoms and solvent molecules are omitted for clarity. (B) Structure of the core of **1**. All hydrogen and carbon atoms and solvent molecules are omitted for clarity.

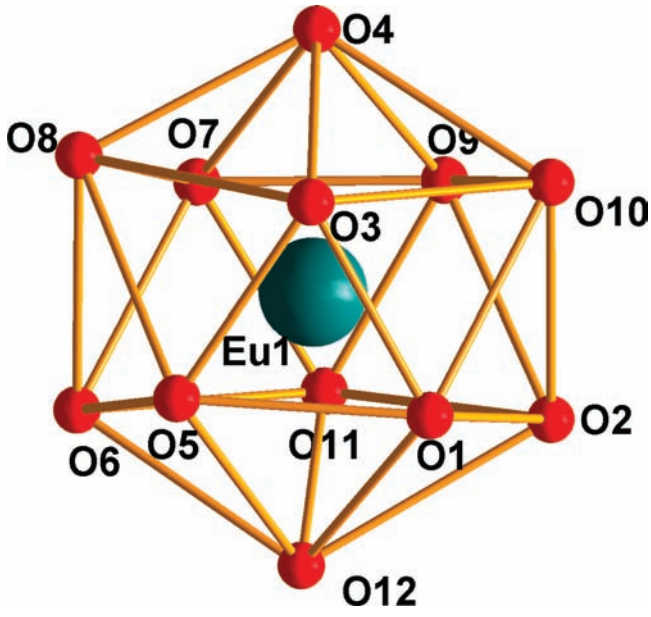

Figure 2. Icosahedral coordination environment around Eu(1) in **1**.

X-Ray Crystal Structures of 1−4. Molecular Structures. Complexes **1**−**4** are isostructural and crystallize in a triclinic unit cell (space group: $P\bar{1}$). The asymmetric unit of **1** contains a {[L_2Co_2Eu][Cl]} unit and two chloroform and one methanol molecule. On the other hand, asymmetric units of **2**, **3**, and **4** contain one-half of the complex and (i) one chloroform and one water molecules for **2** and **3** and (ii) only one chloroform molecule for **4**. The molecular structure of **1** is shown in Figure 1; those of **2**−**4** are given in the Supporting Information. The molecular structures of **1**−**4** reveal that the three metal ions are held together by a concerted coordination action of two trianionic ligands, L^{3-}. The nine coordination sites of each ligand are utilized. The two terminal Co^{II} ions contain a facial coordination environment (3N, 3O) comprising three imino nitrogen atoms and three phenolate oxygen atoms (Figure 1b), inducing a severely distorted coordination geometry around Co^{II} (see the Supporting Information). An *all-oxygen* coordination environment is present around the central lanthanide ion, which is present in a distorted icosahedral geometry (Figure 2). This coordination sphere around the lanthanide ion is achieved by utilizing three phenolate oxygen atoms and three methoxy oxygen atoms of each ligand. Thus, every phenolate oxygen atom acts as a μ-bridging ligand. Three such bridging ligands hold the Co^{II} and Ln^{III} ions together to form the final complexes (see the Supporting Information).

The bond parameters of **1**−**4** are summarized in Table 2. In general, the Co−N bond distances are slightly longer than the Co−O bond distances, although this difference is not large here. Among the Ln−O distances, two types are clearly seen: (i) six are short (~2.4 Å, see Table 2) and involve the $Ln-O_{phenolate}$ bond, and (ii) the other six involving the $Ln-O_{methoxy}$ bond are much longer (~2.9 Å, see Table 2). This is similar to what was observed earlier in {[L_2Co_2Gd][NO_3]}.[12] In all of these trinuclear complexes (**1**−**4**), the Co−Ln distances are around 3.3 Å, while the Co−Co distances range from 6.54 to 6.60 Å.

Table 2. Selected Bond Lengths (Å) and Bond Angles (deg) of Compounds **1**−**4**

	1	**2**[a]	**3**[b]	**4**[c]
P−S	1.9242(2)[d]	1.9317(17)	1.926(2)	1.927(2)
P−N[d]	1.670(4)	1.669(9)	1.663(7)	1.657(7)
N−N[d]	1.448(6)	1.454(12)	1.450(8)	1.448(8)
N═C[d]	1.293(6)	1.299(13)	1.295(9)	1.289(9)
Co−N	2.119(4)	2.101(7)	2.087(6)	2.096(6)
	2.122(4)	2.126(8)	2.106(6)	2.103(6)
	2.158(4)	2.111(8)	2.132(6)	2.127(6)
	2.111(4)	2.113(8)[d]	2.108(6)[d]	2.109(6)[d]
	2.116(4)			
	2.122(4)			
	2.125(4)[d]			
Co−O	2.080(3)	2.077(3)	2.076(4)	2.077(4)
	2.106(3)	2.086(3)	2.092(4)	2.093(4)
	2.118(3)	2.088(3)	2.105(4)	2.107(4)
	2.078(3)	2.084(3)[d]	2.091(4)[d]	2.091(4)[d]
	2.082(3)			
	2.083(3)			
	2.091(3)[d]			
Ln−$O_{phenolic}$	2.399(3)	2.393(3)	2.363(5)	2.364(4)
	2.407(3)	2.396(3)	2.371(4)	2.373(4)
	2.407(3)	2.396(3)	2.390(4)	2.388(4)
	2.408(3)	2.395(3)[d]	2.375(4)[d]	2.375(4)[d]
	2.432(3)			
	2.433(3)			
	2.414(3)[d]			
Ln−$O_{methoxy}$	2.777(3)	2.865(3)	2.878(4)	2.897(4)
	2.857(4)	2.869(3)	2.882(4)	2.898(4)
	2.882(4)	2.875(3)	2.907(4)	2.932(2)
	2.888(3)	2.870(3)[d]	2.889(4)[d]	2.909(4)[d]
	2.889(4)			
	2.908(4)			
	2.867(4)[d]			
Co···Co	6.6685(11)	6.6210(15)	6.5619(13)	6.5384(13)
Co···Ln	3.3312(8)[d]	3.3105(9)	3.2810(8)	3.2692(9)
Co−Ln−Co	177.484(18)	179.99(2)	180.00(2)	180.00(19)

[a] Symmetry operation used to generate equivalent atoms $-x+2, -y, -z+2$. [b] Symmetry operation used to generate equivalent atoms $-x, -y+1, -z+1$. [c] Symmetry operation used to generate equivalent atoms $-x+1, -y+1, -z+1$. [d] Average bond distances.

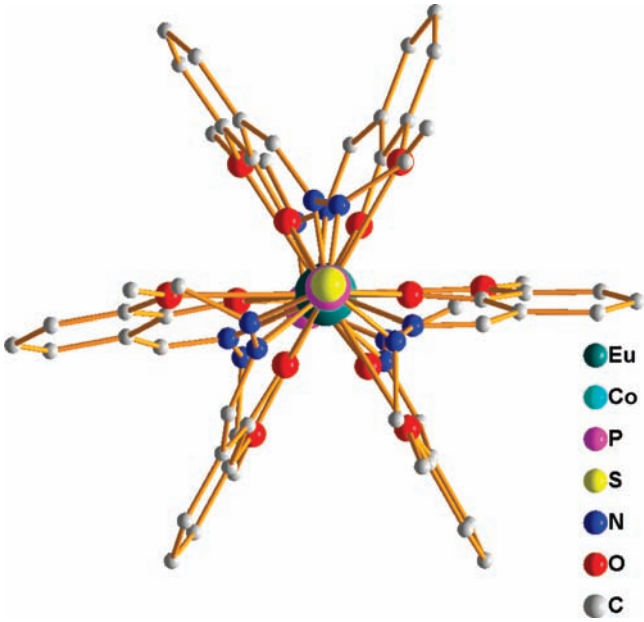

Figure 3. Paddlewheel arrangement of ligands around Co−Ln−Co axis in **1**.

In **2**−**4**, the Co−Ln−Co bond angle is perfectly linear (∼180°), whereas in **1** the Co−Eu−Co bond angle is slightly smaller (177.3°; Table 2). As a result, in all of the compounds, a perfect paddlewheel type of ligand architecture is seen when the molecules are viewed along the Co−Ln−Co axis (Figure 3).

Stereochemistry of the Trinuclear Complexes 1−4. Although the ligand LH_3 is achiral, it induces chirality in the complexes upon complexation. Δ (clockwise) and Λ (anticlockwise) configurations are formed as a result of the screw-type coordination mode imposed by the ligand. This type of behavior was demonstrated by Wieghardt and co-workers earlier and more recently by us.[15−18] In the present case, three chelate rings are formed on either end of the cationic portion of the complex: P−[N−N−C−C−O−Co]$_3$. All of these chelate rings can be oriented in the same direction and can give rise to *λλλ* (all rings oriented clockwise with respect to the intermetal axis) or *δδδ* (all rings oriented anticlockwise with respect to the intermetal axis) (Chart 1).

In all of the cases, we have *always* observed the same conformation for all three rings, and in no instance were mixed conformations such as *λλδ*, *λδλ*, and so forth found. If the conformation is the same at both ends of the trinuclear complex (for example, *λλλ* and *λλλ*), a pure enantiomer is obtained. On the other hand, if the conformation is different at both ends, that is, *δδδ* and *λλλ*, a meso formation would be stabilized. Indeed, both cases are observed experimentally in this family of compounds depending on the Co−Ln−Co angle. While **1**, which has a Co−Eu−Co angle less than 180°, is found to possess *λλλ*−*λλλ* (Δ−Δ) or *δδδ*−*δδδ* (Λ−Λ) forms, **2**−**4**, which contain a Co−Ln−Co bond angle of 180°, crystallize in their meso forms (Δ−Λ; Table S1, Supporting Information).

Another interesting aspect of the stereochemistry of **1**−**4** is the presence of chiral recognition in their supramolecular structures. The crystal structures of **1**−**4** show the presence of C−H···S═P mediated intermolecular interactions to afford a one-dimensional doubly bridged polymeric arrangement. In **1**, among such polymer chains, only molecules with

(14) (a) *SMART Software Reference Manual*; *SAINT Software Reference Manual*, version 6.45; Bruker Analytical X-ray Systems, Inc.: Madison, WI, 2003. (b) Sheldrick, G. M. *SADABS*, version 2.05; University of Göttingen: Göttingen, Germany, 2002. (c) *SHELXTL Reference Manual*, version 6.1; Bruker Analytical X-ray Systems, Inc.: Madison, WI, 2000. (d) Sheldrick, G. M. *SHELXTL*, v.6.12; Bruker AXS Inc.: Madison, WI, 2001. (e) Sheldrick, G. M. *SHELXL97*; University of Göttingen: Göttingen, Germany, 1997.

(15) (a) Beissel, T.; Birkelbach, F.; Bill, E.; Glaser, T.; Kesting, F.; Krebs, C.; Weyhermüller, T.; Wieghardt, K.; Butzlaff, C.; Trautwein, A. X. *J. Am. Chem. Soc.* **1996**, *118*, 12376–12390. (b) Albela, B.; Bothe, E.; Brosch, O.; Mochizuki, K.; Weyhermüller, T.; Wieghardt, K. *Inorg. Chem.* **1999**, *38*, 5131–5138.

(16) (a) Glaser, T.; Beissel, T.; Weyhermüller, T.; Schünemann, V.; Meyer-Klaucke, W.; Trautwein, A. X.; Wieghardt, K. *J. Am. Chem. Soc.* **1999**, *121*, 2193–2208. (b) Glaser, T.; Bill, E.; Weyhermüller, T.; Meyer-Klaucke, W.; Wieghardt, K. *Inorg. Chem.* **1999**, *38*, 2632–2642.

(17) (a) Katsuki, I.; Matsumoto, N.; Kojima, M. *Inorg. Chem.* **2000**, *39*, 3350–3354. (b) Nagasato, S.; Katsuki, I.; Motoda, Y.; Sunatsuki, Y.; Matsumoto, N.; Kojima, M. *Inorg. Chem.* **2001**, *40*, 2534–2540. (c) Katsuki, I.; Motoda, Y.; Sunatsuki, Y.; Matsumoto, N.; Nakashima, T.; Kojima, M. *J. Am. Chem. Soc.* **2002**, *124*, 629–640. (d) Ikuta, Y.; Ooidemizu, M.; Yamahata, Y.; Yamada, M.; Osa, S.; Matsumoto, N.; Iijima, S.; Sunatsuki, Y.; Kojima, M.; Dahan, F.; Tuchagues, J.-P *Inorg. Chem.* **2003**, *42*, 7001–7017. (e) Sunatsuki, Y.; Ohta, H.; Kojima, M.; Ikuta, Y.; Goto, Y.; Matsumoto, N.; Iijima, S.; Dahan, F.; Tuchagues, J.-P. *Inorg. Chem.* **2004**, *43*, 4154–4171.

(18) (a) Chandrasekhar, V.; Azhakar, R.; Zacchini, S.; Bickley, J. F.; Steiner, A. *Inorg. Chem.* **2005**, *44*, 4608–4615.

Chart 1. (a) Molecular Structure of Phosphorus Based Tripodal Ligand LH_3 Possessing C_3 Symmetry, (b) Δ (λλλ) [clockwise] Form of the Configuration Formed by the Ligand LH_3 after Coordination with the Terminal Metal Atom, and (c) Λ (δδδ) [anticlockwise] Form of the Configuration Formed by the Ligand LH_3 after Coordination with the Terminal Metal Atom

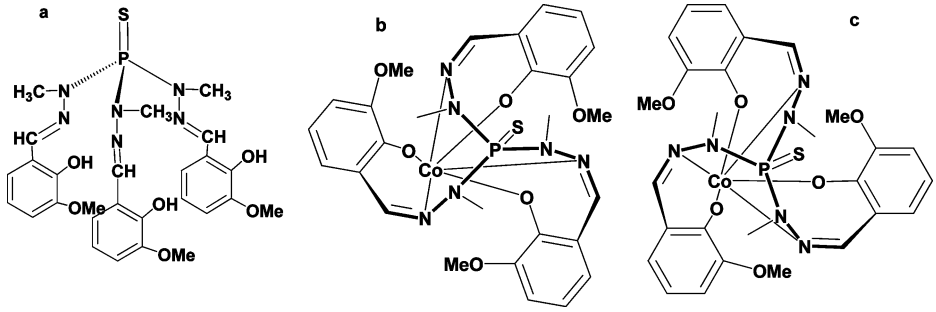

the same configurations interact (i.e., a molecule with a Δ−Δ or Λ−Λ configuration interacts with another molecule possessing a Δ−Δ or Λ−-Λ configuration, respectively; Figure 4). In **2**−**4**, the same trend is observed. A molecule with a Δ−Λ configuration interacts with another molecule possessing a similar configuration (Figure 5). The supramolecular organization is formed as a result of each molecule interacting through the terminal P═S unit with the hydrogen atoms of the aromatic rings of two neighboring molecules. In these weak interactions, the sulfur atom functions as the proton acceptor, while the aromatic C−H group (para to the −OMe group) functions as a proton donor.

Static Magnetic Properties: dc Measurements. Magnetic susceptibility measurements were carried out on polycrystalline samples of **1**, **2**, **3**, and **4** in the temperature range 1.8−300 K at 1000 Oe. The room-temperature χT products estimated at 6.8, 22.1, 23.0, and 18.4 $cm^3 \cdot K/mol$ are in good agreement with the presence of two $S = 3/2$ Co^{II} ions ($S = 3/2$ spin with a Curie constant around 3 $cm^3 \cdot K/mol$) and one lanthanide metal ion: one Eu^{III} ($S = 0$, $^7F_0$) for **1**, one

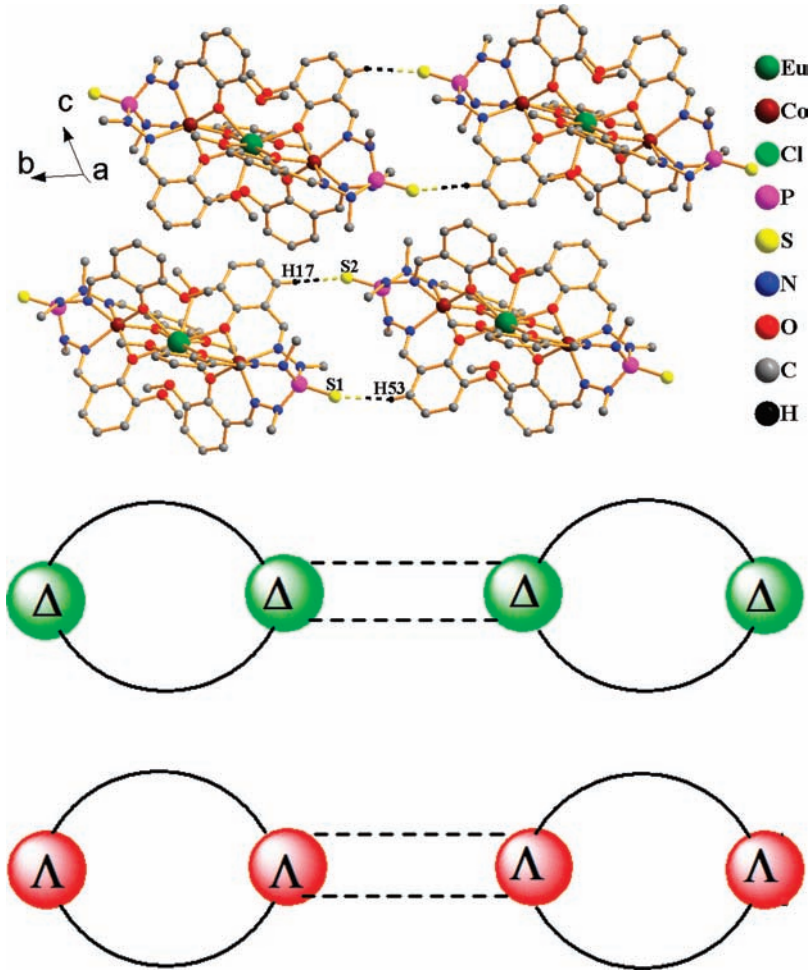

Figure 4. Crystal structure view and scheme of the network made by the intermolecular C−H···S═P hydrogen bonds in **1**. Solvents, chloride anion, and the hydrogen atoms which are not involved in the interaction have been omitted for clarity. The bond parameters for C−H···S═P contacts are S1···H53, 2.7859(16) Å; S1···C53, 3.6874(56) Å; and C53−H53−S1, 158.81(32)° (symmetry is x, $1 + y$, z) and S2···H17, 2.7773(16) Å; S2···C17, 3.6479(55) Å; and C8−H8−S2, 152.76(32)° (symmetry is x, $-1 + y$, z).

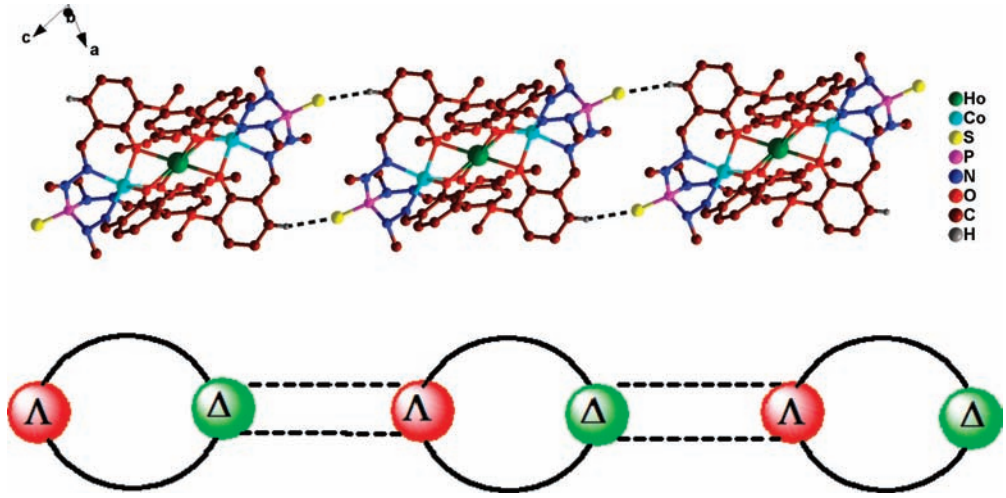

Figure 5. Crystal structure view and scheme of the network made by the intermolecular C−H···S=P hydrogen bonds in **4**. Solvents, nitrate anion, and the hydrogen atoms which are not involved in the interaction have been omitted for clarity. The bond parameters for C−H···S=P contacts are S1···H5, 2.886(4) Å; S1···C5, 3.790(9) Å; and C5−H5−S1, 161.43(47)° (symmetry is $2 - x$, $1 - y$, $-z$).

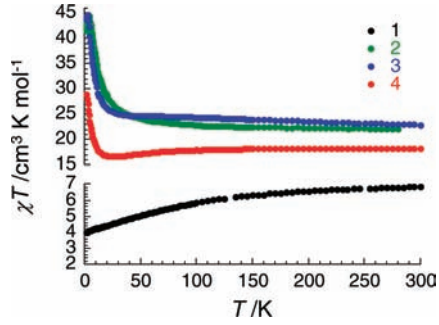

Figure 6. Temperature dependence of the χT product at 1000 Oe for **1**−**4** (with χ = M/H normalized per mol).

Tb^{III} metal ion ($S = 3$, $L = 3$, $^7F_6$ $g = 3/2$: $C = 11.815$ cm^3·K/mol) for **2**, one Dy^{III} metal ion ($S = 5/2$, $L = 5$, $^6H_{15/2}$ $g = 4/3$: $C = 14.17$ cm^3·K/mol) for **3**, and one Ho^{III} ($S = 2$, $L = 6$, $^5I_8$ $g = 5/4$: $C = 14.075$ cm^3·K/mol) for **4**.[19] As shown in Figure 6, the magnetic properties of the four compounds are relatively different when studied as a function of the temperature. When the temperature is decreased, the χT product of **1** at 1000 Oe decreases to reach 3.96 cm^3·K/mol at 1.8 K (Figure 6). On the other hand, the χT product of **2** and **3** at 1000 Oe continuously increases upon lowering the temperature to reach 44.4 and 44.9 cm^3·K/mol, respectively, at 3.4 and 2.5 K, suggesting the presence of dominant ferromagnetic interactions in the trinuclear complexes. At lower temperatures, χT slightly decreases in both cases, probably as the result of magnetic anisotropy or weak antiferromagnetic interaction between trinuclear complexes (Figure 6). In the case of compound **4**, the χT product at 1000 Oe progressively decreases, upon decreasing the temperature, to reach 16.6 cm^3·K/mol at 23 K and then increases to reach a 1.8 K value saturating at 29.2 cm^3·K/mol (Figure 6). It is difficult to analyze the high-temperature susceptibility of these compounds as the presence of Co^{II} and Ln^{III} metal ions with their intrinsic complicated magnetic characteristics makes it very difficult to apply a theoretical approach. Nevertheless, the smooth decrease of χT at high temperatures, observed in **1** and **4**, might have three origins: (i) a progressive depopulation of the Ln^{III} excited states often seen for lanthanide ions when the temperature is lowered, (ii) the presence of spin−orbit coupling, well-known in Co^{II} systems, resulting in the splitting of the energy levels arising from the $^4T_{1g}$ ground term that finally stabilizes a doublet ground state at low temperatures,[20] or (iii) intramolecular antiferromagnetic interactions between Co^{II} and Ln^{III} ions. In this situation, it is very difficult to determine the relative contributions of the magnetic intramolecular interactions versus thermal depopulation of the Stark levels and also versus spin−orbit coupling of the Co^{II} ion in the observed magnetic behavior shown in Figure 6. In the cases of **2** and **3**, all of these effects invoked for **1** and **4**, which tend to decrease the χT product when lowering the temperature, seem to be overcome by intramolecular ferromagnetic interactions that increase the χT product and stabilize a large spin ground state.

The field dependence of the magnetization of these compounds has been measured below 10 K (Figure S4−S7, Supporting Information). For **1**, these magnetization measurements reveal a gradual increase of the magnetization at low fields, in good agreement with the expected low-temperature scheme of two Co^{II} spins weakly interacting through essentially a diamagnetic Eu^{III}. The reverse situation, that is, a relatively steep increase of the magnetization, is observed for the three other compounds in accord with a high-spin ground state for these complexes. At high fields, a progressive saturation of the magnetization that is not completely achieved at 1.8 K under 7 T is observed. The magnetization values under 7 T and at 1.8 K are 4.2, 10.7, 13.0, and 10.0 μ_B for **1**, **2**, **3**, and **4**, respectively. The gradual saturation of the magnetization suggests the possible presence of a magnetic anisotropy or more likely the presence of low-lying excited states expected with the weak Co···Ln magnetic interactions already discussed above. These two magnetic effects are also highlighted by the nonsuperposition

(19) (b) Chandrasekhar, V.; Azhakar, R.; Pandian, B. M.; Bickley, J. F.; Steiner, A. *Eur. J. Inorg. Chem.* **2008**, 1116–1124. Benelli, C.; Gatteschi, D. *Chem. Rev.* **2002**, *102*, 2369–2388.

(20) Carlin, R. L. *Magnetochemistry*; Springer-Verlag: Berlin, 1986.

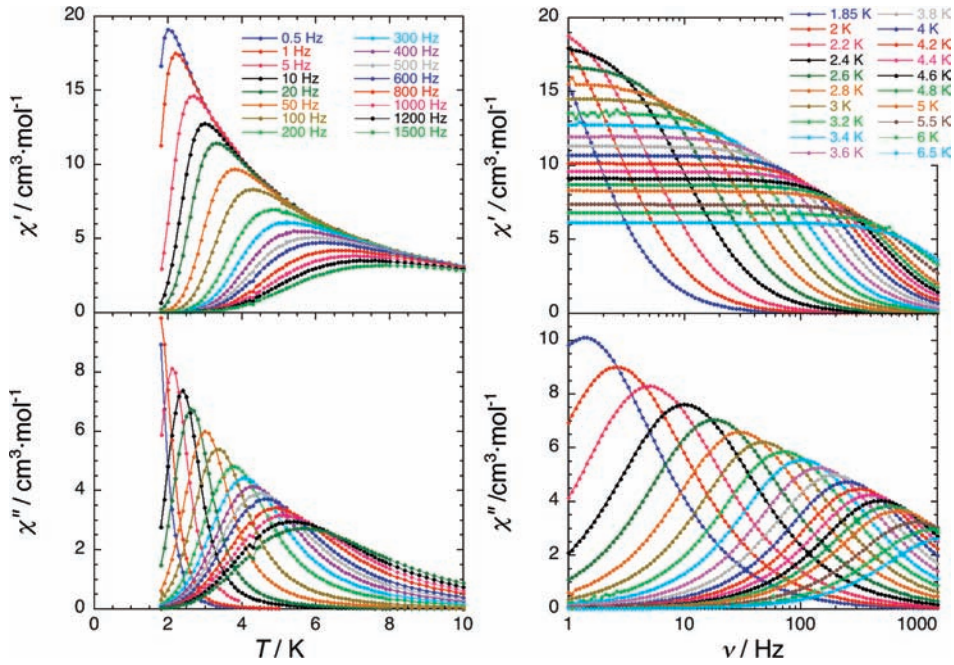

Figure 7. Temperature dependence (left) and frequency dependence (right) of the ac susceptibility for **2** as a function of the temperature below 10 K (left) and the ac frequency between 1 and 1500 Hz (right) under a zero-dc field.

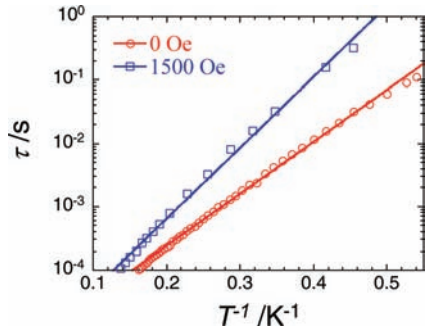

Figure 8. Relaxation time (τ) as a function of T^{-1} at $H_{dc} = 0$ Oe (open red dots) and $H_{dc} = 1500$ Oe (open blue squares) for **2**. The solid lines represent Arrhenius fits of the data discussed in the text.

of the magnetization curves while plotted as a function of H/T (Figures S4−S7, Supporting Information).

Single-Molecule Magnet Properties: ac Measurements. Although at the lowest temperature available (1.8 K), the M versus H data do not show any sign of significant hysteresis effect (i.e., slow relaxation of the magnetization on the time scale of the dc measurements), ac susceptibility as a function of the temperature at different frequencies and also as a function of the frequency at different temperatures has been performed on all the compounds of this family (Figure 7; Figures S8−S17, Supporting Information). While, for **1**, no out-of-phase susceptibility was detected, compounds **2**, **3**, and **4** exhibit amazingly nice dynamic properties compatible with SMM behavior. In order to summarize these results, the dynamics properties for **2** will be described as a representative example. For **3** and **4**, data are given in the Supporting Information in Figures S8−S17. From the obtained data shown in Figure 7 for **2**, the relaxation time (τ) can be determined between 1.8 and 7 K. In this temperature range, τ is thermally activated (Arrhenius like behavior, Figures 8; Figures S10 and S15, Supporting

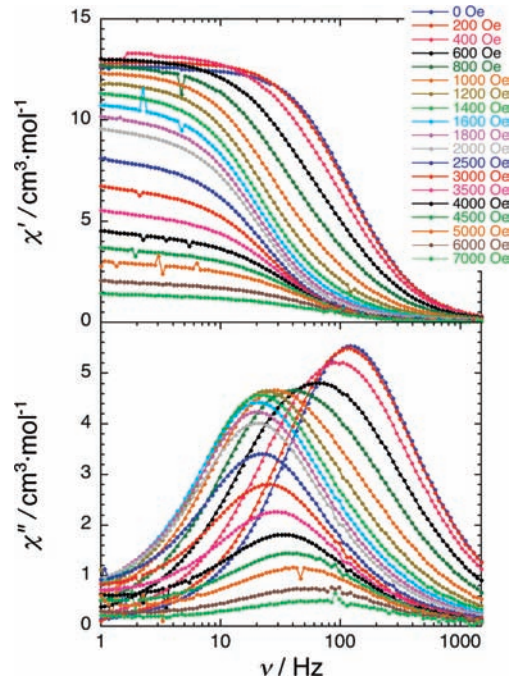

Figure 9. Frequency dependence of the ac susceptibility for **2** as a function of the ac frequency between 1 and 1500 Hz at 3.5 K under dc fields.

Information) with energy barriers of about 18.9, 14.2, and 8 K, while the pre-exponential factors of the Arrhenius laws (τ_0) are 5.5×10^{-6} s, 5.1×10^{-6} s, and 13×10^{-5} s for **2**, **3**, and **4**, respectively.

In order to further study this relaxation time above 1.8 K, the frequency dependence of the ac susceptibility was measured at 3.8 K under a small dc field (Figure 9). Indeed, at temperatures between the thermal and the quantum SMM regimes, quantum effects are expected to still influence the thermally activated relaxation, and thus the energy gap (Δ) of the Arrhenius law is reduced by the quantum tunnelling

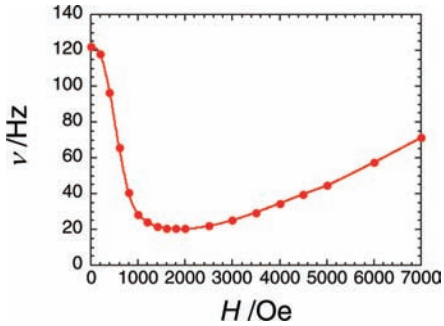

Figure 10. Field dependence of the characteristic frequency at 3.5 K for **2** deduced from Figure 9.

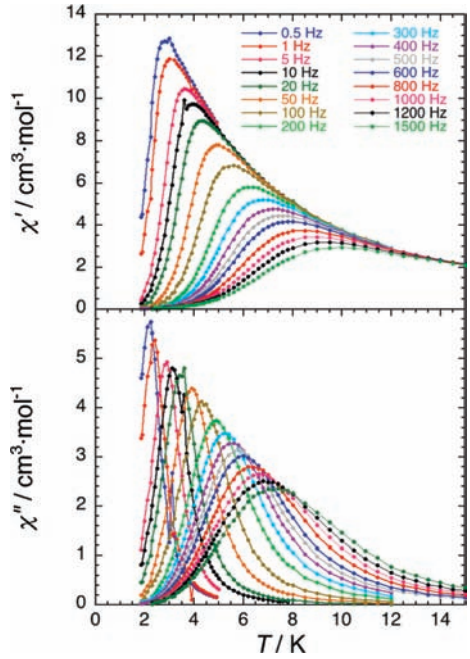

Figure 11. Temperature dependence of the ac susceptibility for **2** as a function of temperature below 15 K under 1500 Oe.

of the excited states. Experimentally, Δ takes an effective value, and thus the observed relaxation time becomes faster. Therefore, in order to study only the thermal relaxation in this regime, a small dc field can be applied to remove the degeneracy of the m_S states, lowering the probability of the zero-field QTM between the $\pm m_S$ states.[10a,21] As expected in presence of significant quantum effects, the application of a small dc field slows down the relaxation for **2**; that is, the relaxation mode is going down in frequency with an increasing dc field (Figures 9 and 10). While in zero field, the characteristic frequency is 122 Hz at 3.5 K, and it decreases to reach 20 Hz around an optimum field of 1500 Oe. It is worth mentioning that the same type of ac measurements under dc fields have been done for **3** and **4** (Figures S11-S12 and S16-S17, Supporting Information) and that, even at low fields, the relaxation time become faster than in zero field, indicating the absence, or the negligible influence, of the quantum effects at 3 K for these compounds.

As shown in Figure 11 for compound **2**, the slow relaxation is significantly moved at higher temperatures under small dc fields: for example, at 1500 Hz, the blocking temperature is increased from 5.7 to 7.3 K when increasing the dc field from 0 to 1500 Oe. The deduced activated behavior of the relaxation time based on the 1500 Oe dc field measurements (Figure 11) is shown Figure 8. The fit of these data by the Arrhenius law leads to a characteristic SMM energy gap, Δ, estimated at 25.8 K and the pre-exponential factor, τ_0, at 3.7×10^{-6} s. As expected, the application of the small dc field (here 1500 Oe) reduces the quantum relaxation and thus increases the experimental energy gap, becoming closer to the thermal barrier of the ground state.

Concluding Remarks

In conclusion, we have assembled a new family of 3d−4f compounds containing Co^{II}. A specially designed phosphorus-supported multidentate ligand, LH_3 {LH_3 = (S)P[N(Me)N=CH−C_6H_3-2-OH-3-OMe]$_3$} containing nine coordination sites in the form of three imino nitrogen atoms, three phenolate oxygen atoms, and three methoxy oxygen atoms, has allowed the preparation of linear heterometallic trinuclear complexes {[L_2Co_2Ln][X]}; Ln = Eu, X = Cl (**1**); Ln = Tb, X = NO_3 (**2**); Ln = Dy, X = NO_3 (**3**); Ln = Ho, X = NO_3 (**4**)]. All of these compounds are isostructural, and the cationic portion of the complexes contains a linear Co−Ln−Co arrangement. The central lanthanide metal ion is surrounded by 12 oxygen atoms and possesses a distorted icosahedral geometry. The two terminal cobalt atoms are hexa-coordinate containing a facial 3N, 3O coordination environment. Detailed magnetic studies on these complexes reveal that **2**, **3**, and **4** are single-molecule magnets, while the Eu analogue does not display such properties. The modular nature of the ligand LH_3 allows subtle changes to be made without affecting its overall coordination behavior. Currently, we are exploring these possibilities with a view to examining their effect on the SMM energy gaps, relaxation rates, and blocking temperatures.

Acknowledgment. We thank the Department of Science and Technology, India, and Council of Scientific and Industrial Research, India, for financial support. V.C. is a Lalit Kapoor Chair Professor of Chemistry. V.C. thanks the Department of Science and Technology, for a J.C. Bose fellowship. B.M.P. thanks Council of Scientific and Industrial Research, India, for a Senior Research Fellowship. R.C. thanks the Conseil Régional d'Aquitaine, the Université de Bordeaux, and the CNRS for financial support.

Supporting Information Available: Figures S1−S18 and Table S1: Diamond pictures of compounds **2**−**4** and additional magnetic measurement on compounds **1**−**4**. This material is available free of charge via the Internet at http://pubs.acs.org.

IC801905P

(21) (a) Li, D.; Clérac, R.; Parkin, S.; Wang, G.; Yee, G. T.; Holmes, S. M. *Inorg. Chem.* **2006**, *45*, 5251–5253. (b) Martínez-Lillo, J.; Armentano, D.; Munno, G. D.; Werndorfer, W.; Julve, M.; Lloret, F.; Faus, J. *J. Am. Chem. Soc.* **2006**, *128*, 14218–14219. (c) Poneti, G.; Bernot, K.; Bogani, L.; Caneschi, A.; Sessoli, R.; Wernsdorfer, W.; Gatteschi, D. *Chem. Commun.* **2007**, 1807–1809. (d) Ako, A. M.; Mereacre, V.; Hewitt, E. J.; Clérac, R.; Lecren, L.; Anson, C. E.; Powell, A. K. *J. Mater. Chem.* **2006**, *16*, 2579–2586. (e) Kachi-Terajima, C.; Miyasaka, H.; Saitoh, A.; Shirakawa, N.; Yamashita, M.; Clérac, R. *Inorg. Chem.* **2007**, *46*, 5861–5872.